Wärme- und Stoffübertragung 23, 249–257 (1988)

Wärme- und Stoffübertragung

Analysis of fully developed opposing mixed convection between inclined parallel plates

A. S. Lavine, Los Angeles, CA, USA

Abstract. An exact solution is presented of fully developed, laminar flow between inclined parallel plates with a uniform wall heat flux boundary condition. The flow is downward and the heat flux is into the channel, so that natural convection opposes the forced flow. The solution depends on the two parameters $P_1 = Gr \sin\theta/Re$ and $P_2 = Gr \cos\theta/Re^2 Pr$. Four different flow reversal regimes are observed: 1) no reversal, 2) top reversal, 3) bottom reversal, and 4) top and bottom reversal. Velocity profiles, temperature profiles, wall friction, and Nusselt numbers are presented. Despite the simplicity of the problem which has been analyzed, it does display some features which have been observed in real mixed convection flows, such as flow reversal and nonmonotonic dependence on tilt angle.

Berechnung der voll entwickelten entgegengesetzt gerichteten Misch-Konvektion zwischen geneigten parallelen Platten

Zusammenfassung. Es wird eine exakte Lösung für voll entwickelte laminare Strömung zwischen geneigten parallelen Platten mit einheitlichem Wand-Wärmestrom als Randbedingung dargestellt. Die Strömung ist abwärts gerichtet und der Wärmestrom führt in den Kanal, so daß die freie Konvektion der erzwungenen entgegengesetzt gerichtet ist. Die Lösung hängt von den beiden Parametern $P_1 = Gr \sin\theta/Re$ und $P_2 = Gr \cos\theta/Re^2 Pr$ ab. Vier verschiedene Bereiche der Strömungsumkehr wurden betrachtet: 1) keine Richtungsumkehr, 2) Umkehr an der Oberseite, 3) Umkehr an der Unterseite und 4) Umkehr an Ober- und Unterseite. Es wurden Geschwindigkeits- und Temperaturprofile, Wandreibung und Nusselt-Zahlen dargestellt. Trotz der Einfachheit des analysierten Problems werden einige Dinge dargestellt, welche in realer gemischter Konvektion untersucht wurden, so z. B. Strömungsumkehr und die nicht-monotone Abhängigkeit vom Schrägungswinkel.

Nomenclature

f	friction factor $= \tau_w/(\frac{1}{2}\varrho_0 \bar{u}^2)$
g	gravitational acceleration constant $= 9.8\ m/s^2$
Gr	Grashof number $= g\beta q L^4/k\nu^2$
k	fluid thermal conductivity
L	channel width
m	$= (2P_1)^{0.25}$
Nu	Nusselt number $= 2qL/k(T_w - T_b)$
p	fluid thermodynamic pressure
P	nondimensional pressure $= [p - \varrho_0 g(x \sin\theta - y \cos\theta)]/Pr\,\varrho_0 \bar{u}^2$
Pr	Prandtl number $= \nu/\alpha$
P_1	$= Gr \sin\theta/Re$
P_2	$= Gr \cos\theta/Re^2 Pr$
q	wall heat flux
Re	Reynolds number $= \bar{u}L/\nu$
T	fluid temperature
T_b	fluid bulk temperature
T_0	constant reference temperature
T_w	fluid temperature
u	axial velocity
$\bar{u}$	average velocity
U	nondimensional velocity $= u/\bar{u}$
x	axial coordinate
X	nondimensional axial coordinate $= x\alpha/\bar{u}L^2$
y	transverse coordinate
Y	nondimensional transverse coordinate $= y/L$
α	fluid thermal diffusivity
β	fluid thermal expansion coefficient
θ	tilt angle, measured counterclockwise from horizontal in Fig. 1
ν	fluid kinematic viscosity
ϱ_0	fluid density evaluated at T_0
τ_w	wall shear stress
ϕ	nondimensional temperature $= (T - T_0)/(qL/k)$
ϕ_b	nondimensional bulk temperature $= \int_0^1 U\phi\, dY$
ϕ_w	nondimensional wall temperature $= (T_w - T_0)/(qL/k)$

1 Introduction

Mixed convection in ducted flow may occur in many applications, such as in heat exchangers, chemical processing equipment, transport of heated or cooled fluids, solar collectors, and microelectronic cooling. Flow reversals have been observed to occur near the duct wall when buoyancy opposes the forced flow, or near the duct centerline when buoyancy aids the forced flow. These flow reversals are of substantial significance because they may strongly affect wall friction, pressure drop, heat transfer, occurrence of extreme temperatures, and stability of the flow.

This paper presents an exact solution for laminar, fully developed, opposing mixed convection flow between inclined parallel plates. The problem is highly idealized, and in fact laminar flow would not exist under some of the conditions considered. Nonetheless, the solution does provide insight into phenomena which occur in more realistic opposing mixed convection flows. For instance, the solution is

shown to depend nonmonotonically on inclination angle, and the conditions under which flow reversals occur are determined.

Mixed convection in ducts and channels has received a great deal of attention in the literature. The majority of the work has addressed either the vertical or the horizontal configuration. The case of fully developed mixed convection between horizontal parallel plates with a linear axial temperature distribution was solved by Gill and Del Casal [1]. Ostrach [2] solved the problem of fully developed mixed convection between vertical parallel plates with and without heat sources. Cebeci et al. [3] performed numerical calculations of developing laminar mixed convection between vertical parallel plates for both aiding and opposing conditions. Wirtz and McKinley [4] conducted an experimental study of opposing mixed convection between vertical parallel plates with one plate heated and the other adiabatic. In all of these studies flow reversal was observed under some conditions.

There have been a variety of experimental, analytical, and numerical investigations of opposing mixed convection in vertical pipes [5–9]. Flow reversals were predicted and were observed experimentally.

Mixed convection in inclined geometries has not been studied as exhaustively as for vertical and horizontal configurations. Most of the studies which have been conducted are for aiding flow. Bohne and Obermeier [10] performed an experimental investigation of aiding *and* opposing mixed convection in an inclined cylindrical annulus. Lavine et al. [11, 12] performed an experimental investigation of the opposing case, for a circular pipe. These three studies indicate that some aspects of the flow behavior depend nonmonotonically on tilt angle. The simple opposing mixed convection flow addressed in this paper does display this feature.

2 Problem description

The problem to be solved is that of fully developed, laminar flow between inclined parallel plates with a uniform wall heat flux boundary condition (Fig. 1). The flow is downward and the heat flux is into the channel, so that natural convection opposes the forced flow. For simplicity, only the case of equal heat fluxes at the upper and lower walls will be considered. The assumption of fully developed flow means that the axial (x-direction) velocity depends only on the transverse coordinate, y. Then from continuity, the transverse velocity component must be zero. The temperature is assumed to be a function of x plus a function of y. No assumptions are made with regard to the pressure variation (and in fact it is found *not* to be a linear function of x, as is often assumed). The flow is then described by the following nondimensional equations and boundary conditions, where it has been further assumed that the flow is steady-state and incompressible, with constant properties and negligible viscous dissipation, and that the Boussinesq approximation holds.

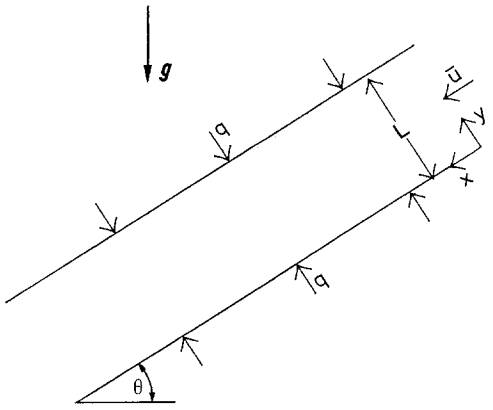

Fig. 1. The parallel plate configuration

$$\frac{\partial P}{\partial X} = -P_1 \phi + \frac{d^2 U}{dY^2}, \tag{1}$$

$$\frac{\partial P}{\partial Y} = P_2 \phi, \tag{2}$$

$$U \frac{\partial \phi}{\partial X} = \frac{\partial^2 \phi}{\partial Y^2}, \tag{3}$$

$$\int_0^1 U \, dY = 1, \tag{4}$$

$$U(0) = U(1) = 0, \quad -\left.\frac{\partial \phi}{\partial Y}\right|_0 = \left.\frac{\partial \phi}{\partial Y}\right|_1 = 1. \tag{5}$$

Integrating Eq. (3) over the channel cross-section, and making use of Eq. (4), the boundary conditions for ϕ, and the assumption that the temperature is a function of x plus a function of y, it can be shown that:

$$\frac{\partial \phi}{\partial X} = 2. \tag{6}$$

These equations have been made nondimensional in such a way that the solution depends only on the two parameters P_1 and P_2, not independently on the four fundamental parameters Re, Gr, Pr, and the tilt angle θ. The parameters P_1 and P_2 are defined as $P_1 = Gr \sin\theta / Re$ and $P_2 = Gr \cos\theta / Re^2 \, Pr$. (Choudhury and Patankar [13] used essentially the same parameters for developing aiding mixed convection in a pipe.) Note that the case of upward flow with cooled walls (also an opposing flow) would correspond to negative values of Gr and θ, so that P_1 would remain positive, while P_2 would become negative. The solution would be identical to the case considered here, except that the velocity and temperature profiles would be reflected about the channel centerline. For instance, when the downward, heated flow exhibits flow reversal at the upper wall, the upward, cooled flow would exhibit reversal at the lower wall.

It is possible, of course, to make use of some different pair of parameters which are a combination of P_1 and P_2, such as replacing P_1 or P_2 with $P_3 = P_1/P_2 = Re \, Pr \tan\theta$. The advantage to doing so is that the Grashof number dependence can then

be isolated in one parameter. However, the pair of parameters P_1, P_2 has the desirable feature that the limits of horizontal and vertical channel flow can be recovered as P_1 goes to zero and P_2 goes to zero, respectively. If P_1 and P_3 had been used, then it would be difficult to recover the horizontal limit, since both P_1 and P_3 go to zero as θ goes to zero (and the solution depends on their ratio, P_2). Furthermore, if the pair P_2, P_3 had been used, it would be difficult to recover the vertical limit, since P_2 goes to zero and P_3 goes to infinity as θ goes to 90 degrees (and the solution depends on their product, P_1). It should also be noted that the forced convection limit is obtained as P_1 and P_2 both go to zero. The case of natural convection corresponds *not* to $Re = 0$, but rather to the situation in which there is no imposed pressure gradient. There would be a net flow in the upward (negative x) direction. This limit cannot be recovered from the solution which will be presented here because the character of the solution changes when Re is negative (i.e. P_1 negative). The aiding mixed convection case (Gr or θ negative) cannot be recovered for the same reason. Finally, it should be noted that the θ dependence necessarily appears in both parameters, and cannot be accounted for simply by multiplying the Grashof number by $\sin\theta$.

3 Results and discussion

The solution to the above equations can be found by differentiating Eqs. (1) and (2) with respect to Y and X respectively, and equating them. Differentiating the resulting equality once more with respect to Y yields $d^4U/dY^4 = P_1\,\partial^2\phi/\partial Y^2$. Then making use of Eqs. (3) and (6) yields $d^4U/dY^4 = 2P_1 U$. This differential equation can be solved for U, and then ϕ and P can be determined. The solution is:

$$U = a[\sinh(mY) + \sin(\mathrm{mY})] + b[\cosh(mY) - \cos(mY)] + m\left(\frac{1}{2} - \frac{P_2}{P_1}\right)\sin(mY), \quad (7)$$

$$\phi = \frac{2}{m^2}\left\{a[\sinh(mY) - \sin(mY)] + b[\cosh(mY) + \cos(mY)] - m\left(\frac{1}{2} - \frac{P_2}{P_1}\right)\sin(mY)\right\} - 2\frac{P_2}{P_1}Y + 2X + A, \quad (8)$$

$$P = m\frac{P_2}{P_1}\left\{a[\cosh(mY) + \cos(mY)] + b[\sinh(mY) + \sin(mY)] + m\left(\frac{1}{2} - \frac{P_2}{P_1}\right)\cos(mY)\right\} + P_2\left(2XY + AY - \frac{P_2}{P_1}Y^2\right) - P_1(AX + X^2) + B \quad (9)$$

where A and B are constants (dependent on P_1 and P_2) chosen such that the initial conditions for ϕ and P are satisfied. The quantity m satisfies $m^4 = 2P_1$, and the constants a and b are the solutions of:

$$a[\sinh(m) + \sin(m)] + b[\cosh(m) - \cos(m)] = -m\left(\frac{1}{2} - \frac{P_2}{P_1}\right)\sin(m), \quad (10)$$

$$a[\cosh(m) - \cos(m)] + b[\sinh(m) - \sin(m)] = m\left(\frac{1}{2} + \frac{P_2}{P_1}\right) + m\left(\frac{1}{2} - \frac{P_2}{P_1}\right)\cos(m). \quad (11)$$

The solution for the horizontal case ($P_1 = 0$) can be found by expanding the above solution for small m, or more simply, by solving the equations from scratch for $P_1 = 0$ [1].

The wall friction and Nusselt number will also be discussed. They are given by:

$$fRe = \frac{\tau_w}{\frac{1}{2}\varrho_0\bar{u}^2}\frac{\bar{u}L}{\nu} = \pm 2\left.\frac{du}{dy}\right|_{0,L} = \pm 2\left.\frac{dU}{dY}\right|_{0,1} \quad (12)$$

where the plus and minus signs correspond to the bottom and top walls, respectively. Then

$$fRe = \begin{cases} 2m\left[2a + m\left(\frac{1}{2} - \frac{P_2}{P_1}\right)\right] & \text{at } Y = 0 \\ -2m\left\{a[\cosh(m) + \cos(m)] + b[\sinh(m) + \sin(m)] + m\left(\frac{1}{2} - \frac{P_2}{P_1}\right)\cos(m)\right\} & \text{at } Y = 1 \end{cases} \quad (13)$$

and

$$Nu = \frac{2qL}{k(T_w - T_b)} = \frac{2}{(\phi_w - \phi_b)} \quad (14)$$

where

$$\phi_b = \int_0^1 U\phi\,dY \quad \text{and} \quad \phi_w = \phi(Y = 0, 1). \quad (15)$$

The average of the top and bottom wall friction is also of interest. It is given by:

$$\overline{fRe} = 0.5[\mathrm{f\,Re}(Y = 0) + fRe(Y = 1)] = m^2\frac{[\cos(m) - \cosh(m) - \sin(m)\sinh(m)]}{\cos(m)\cosh(m) - 1}. \quad (16)$$

Thus, the average wall friction is seen to be independent of the parameter P_2.

3.1 Flow reversal regimes

Starting from forced convection flow, and increasing buoyancy effects (say by increasing the wall heat flux), flow reversal will first occur at the top wall, since thermal stratification causes the fluid to be hottest there. The condition for the onset of flow reversal at the upper wall is $(dU/dY)|_1 = 0$, or fRe at $Y = 1$ (as given by Eq. (13)) equal to zero. This yields the following relationship between P_1 and P_2 for the onset of flow reversal at the upper wall:

$$P_2 = \frac{P_1}{2}\frac{\cos(m) - \cosh(m) - \sin(m)\sinh(m)}{\cos(m) - \cosh(m) + \sin(m)\sinh(m)} \quad (17)$$

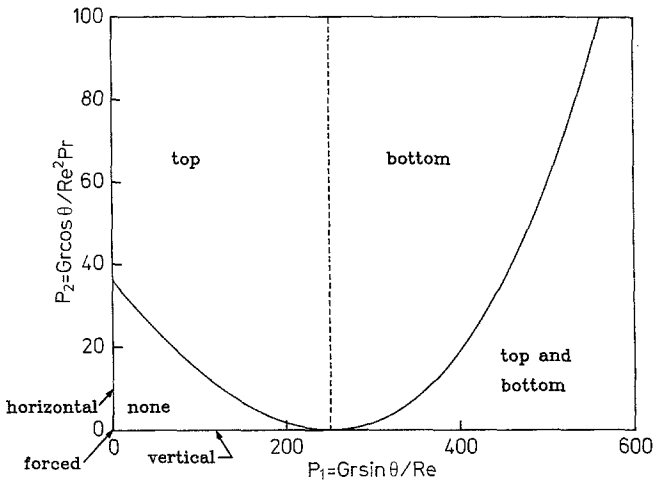

Fig. 2. Flow regime map

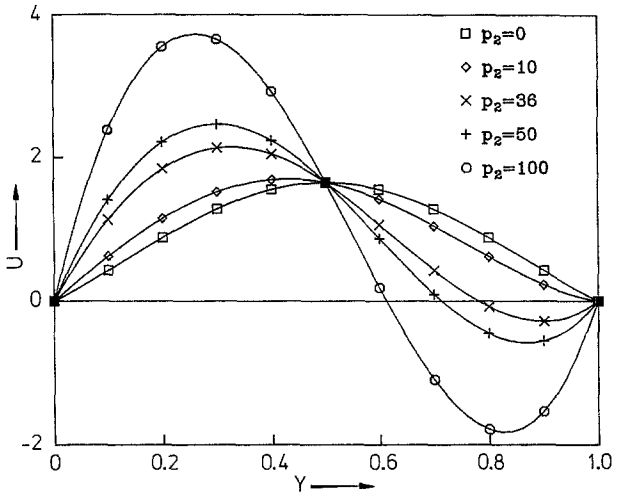

Fig. 3. Velocity profiles, $P_1 = 100$

where it should be recalled that $m^4 = 2P_1$. This curve has been plotted in Fig. 2 (solid line). (The dashed line at $P_1 = 250$ will be discussed shortly.) As P_1 increases beyond the range of the graph, the curve goes through maxima and minima, and flow regimes occur which have multiple reversal regions within the cross-section. However, these regimes have not been investigated due to the likelihood that they would not be observed in reality. Returning to the range shown on the graph, the portion of the curve for $P_1 < 250$ separates the no flow reversal regime from the regime for which reversal occurs at the top wall only. This transition has already been discussed, and is to be expected. The significance of that portion of the curve for which $P_1 > 250$ is less obvious. This curve separates a regime of reversal at the top and bottom walls from a regime of reversal at the bottom wall only. The existence of a regime in which reversal occurs at the top and bottom walls is to be expected: For a vertical channel the flow is symmetric about the channel centerline, so that when flow reversal occurs it must occur at both walls. Thus it is reasonable to expect flow reversal at both the top and bottom walls for some range of parameters for an inclined channel, as well. The regime in which flow reversal occurs only at the bottom wall is somewhat unexpected. What is especially surprising is the nature of the transition from top wall reversal to bottom wall reversal (dashed line). As P_1 is increased from zero, flow reversal first appears at the top wall, and the reversal strength grows (i.e. the magnitude of the negative velocity increases and the reversal encompasses more of the channel cross-section). The wall friction approaches plus and minus infinity at the bottom and top walls, respectively, as P_1 approaches a constant value of approx. 250. At this value of P_1, a discontinuous change occurs in the velocity profile: the reversal at the top wall disappears and a reversal appears at the bottom wall. Of course such an event would not occur in reality, but this aspect of the solution may suggest the occurrence of instability in a real system. Mathematically, what is happening is that the denominator of the constants a and b (Eqs. (10) and (11)), namely $[\cosh(m)\cos(m) - 1]$, is going to zero. The first nonzero root occurs for $m = 4.73$, or $P_1 = 250.2819508$ (to ten significant digits).

Figure 2 also indicates the occurrence of flow reversal at the upper wall in a horizontal channel ($P_1 = 0$), for $P_2 > 36$. This same result was found by Gill and Del Casal [1]. It may seem peculiar that flow reversal is predicted for a horizontal channel, since there is no buoyancy force acting in the axial direction. However, it is the sum of the axial buoyancy force and the axial pressure gradient which determines the axial velocity. The axial pressure gradient can be locally positive (i.e. opposing the main flow) in the upper region of the channel. This occurs for the following reason. The pressure variation in the y-direction is hydrostatic, and $\partial p/\partial y$ is therefore negative. Since the temperature increases with x (and the density therefore decreases with x), $\partial p/\partial y$ becomes less negative, that is, it increases with x. If $\partial p/\partial y$ increases with x then $\partial p/\partial x$ must increase with y. If this effect is extreme enough, then $\partial p/\partial x$ may actually be positive in the upper portion of the channel. The result is a flow reversal at the upper wall, for $P_2 > 36$. In reality, mixed convection in a horizontal channel will be unstable if the Rayleigh number exceeds a critical value. In order for P_2 to exceed 36 while the Rayleigh number remains below its critical value, the parameter $RePr$ must be small. Under realistic conditions, flow reversal would probably not be observed in a horizontal channel.

3.2 Velocity and temperature profiles

Velocity and temperature profiles will now be presented in Figs. 3–6. The temperature profiles will be given as $\phi - \phi_b$, to eliminate the x-dependence of the temperature. Each graph is for a constant value of P_1, with P_2 as a parameter; in other words, for points along a vertical line in the flow regime map, Fig. 2. Figures 3 and 4 show velocity and tem-

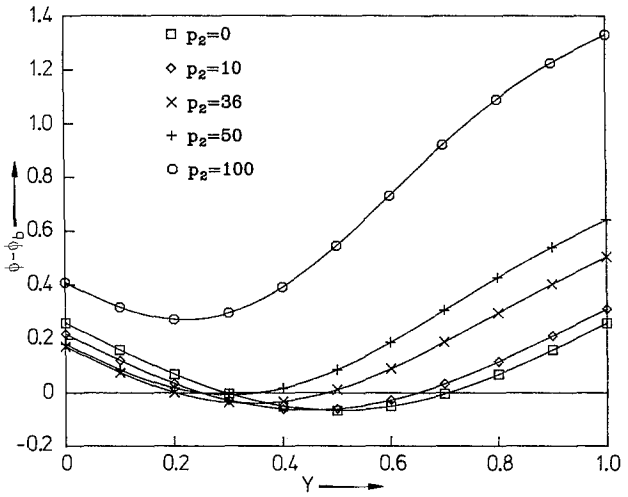

Fig. 4. Temperature profiles, $P_1 = 100$

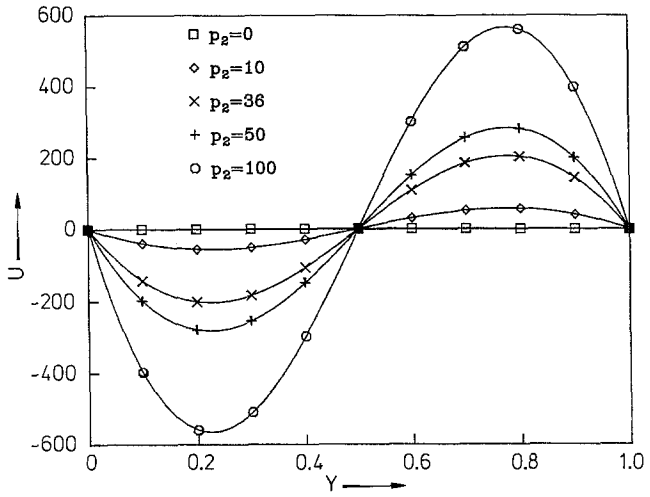

Fig. 5. Velocity profiles, $P_1 = 251$

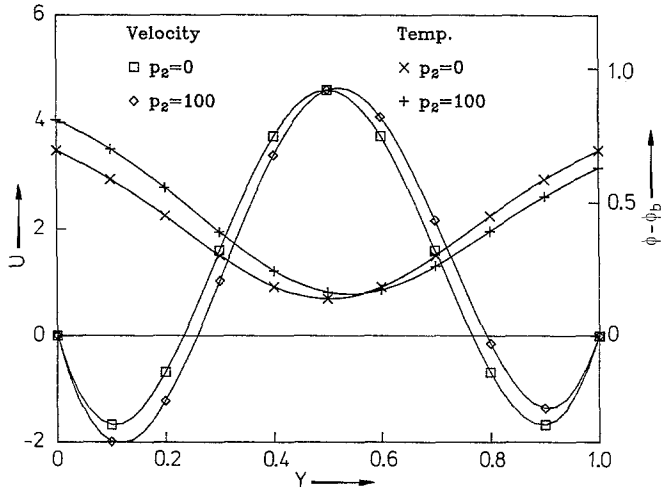

Fig. 6. Velocity and temperature profiles, $P_1 = 1000$

perature profiles for $P_1 = 100$. For $P_2 = 0$ (vertical channel), the velocity profile is symmetric about the centerline. As P_2 increases, the velocity near the upper wall ($Y = 1$) decreases, and the velocity peak increases in magnitude and shifts toward the lower wall ($Y = 0$). Ultimately, flow reversal occurs near the upper wall. In Fig. 4, the temperature at the upper wall is seen to be greater than the temperature at the lower wall, and as P_2 increases the temperature difference between the two walls increases. Note that it is possible for the temperature to be everywhere greater than the bulk temperature, because the velocity is negative over part of the channel cross-section.

As P_1 increases, the following trends are observed: Flow reversal is initiated for lower and lower values of P_2 (Fig. 2). The flow reversals encompass more of the channel cross-section (but never more than the top half). The maximum and minimum values of the velocity profile increase in magnitude, and the cross-sectional temperature variation becomes larger. As P_1 approaches the critical value of 250 (from below), the flow reversal encompasses the entire top half of the channel, the velocity extrema go to plus and minus infinity, and the temperature difference between the top and bottom walls also goes to infinity (with the top wall hotter).

At the critical P_1 value of 250, a discontinuous change occurs from top flow reversal to botttom flow reversal, with the temperature hotter at the *bottom* wall. Figure 5 shows the velocity profiles for $P_1 = 251$, just beyond the transition to the bottom flow reversal regime. The nature of these profiles is opposite to those for $P_1 < 250$, as described above. In Fig. 5, the magnitudes of the velocities are seen to be extremely large. The magnitudes of the temperatures (not shown) are also very large. For instance, for $P_1 = 251$ and $P_2 = 100$, the nondimensional temperature varies from 26,900 at the bottom wall to 26,700 at the top wall. As P_1 increases beyond the value of 250, the velocity and temperature magnitudes decrease.

Figure 6 shows the velocity and temperature profiles for $P_1 = 1000$, corresponding to the top and bottom flow reversal regime. The transition to this regime from the bottom only reversal regime is continuous, with flow reversal gradually appearing at the upper wall and strengthening. The reversal at the top wall is seen to still be smaller than the reversal at the bottom wall for the case shown. Similarly, the fluid is still somewhat hotter at the bottom wall. These graphs also illustrate another feature of the solution, namely that as P_1 approaches infinity, the solution becomes independent of P_2.

3.3 Wall friction and heat transfer

Figure 7 shows the wall friction (in terms of fRe) at the bottom and top walls. The wall friction is plotted as a function of P_1, with P_2 as a parameter. For $P_2 = 0$ (vertical channel), the wall friction is the same at both walls. For $P_1 = P_2 = 0$, fRe is 12 at both walls, corresponding to the

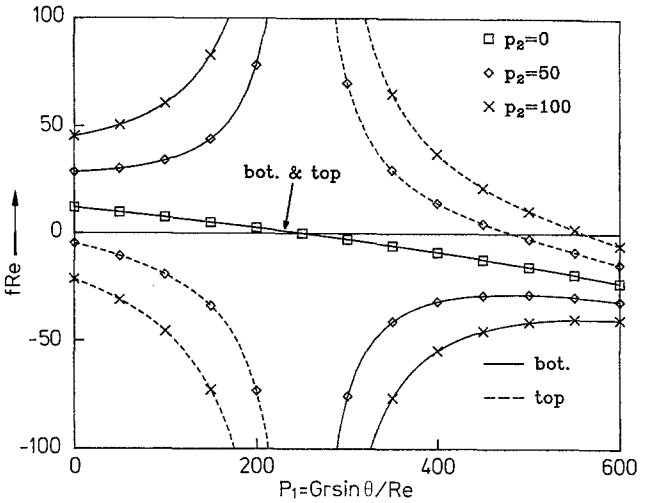

Fig. 7. fRe at top and bottom plates vs. P_1

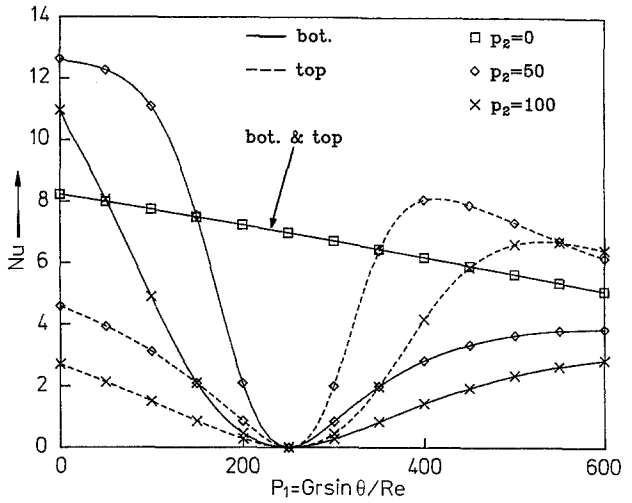

Fig. 8. Nu at top and bottom plates vs. P_1

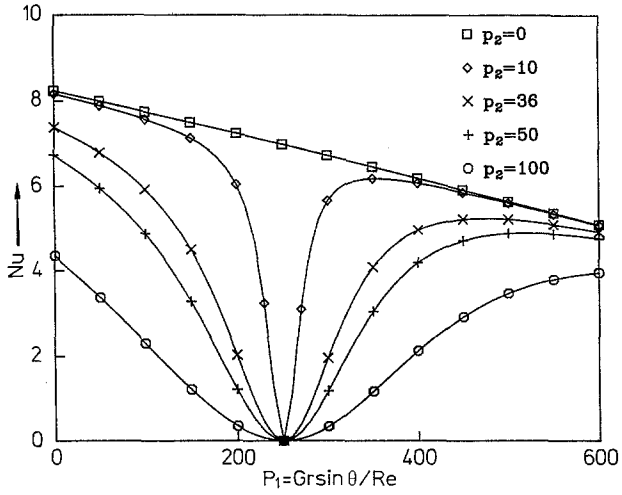

Fig. 9. Average Nu vs. P_1

forced convection solution. As P_1 increases, with P_2 still equal to zero, the wall friction decreases, and becomes negative when flow reversal ensues at $P_1 = 250$. For nonzero P_2, however, the behavior of the wall friction is much different. As explained previously, the wall friction at the lower wall increases, approaching infinity as P_1 goes to 250, while the wall friction at the upper wall decreases toward minus infinity. This corresponds to the strengthening of the flow reversal at the upper wall, and the consequent acceleration near the lower wall. When P_1 becomes greater than 250, the wall friction changes sign, and returns from plus or minus infinity. This of course corresponds to flow reversal at the bottom wall. As P_1 increases, the wall friction becomes negative at both walls, corresponding to the top and bottom flow reversal regime.

Since the top and bottom wall friction are the same for $P_2 = 0$, they are also equal to the *average* wall friction, $\overline{fRe}$. Recall that $\overline{fRe}$ (given by Eq. (16)) is independent of P_2, despite the fact that the top and bottom wall friction are each separately dependent on P_2. Thus, the curve for $P_2 = 0$ in Fig. 7 is also the curve for $\overline{fRe}$ for *any* value of P_2 (i.e., it is Eq. (16)). Note that $\overline{fRe}$ goes to zero at the critical value of $P_1 = 250$, while the top and bottom wall friction are going to plus and minus infinity (for nonzero P_2). Thus, for $P_1 = 250$, the total axial buoyancy force is exactly balanced by the total axial pressure force (where "total" implies an integral over the cross-section). For $P_1 > 250$, the average wall friction is negative. The pressure force required to drive the flow would then be less than the axial buoyancy force.

Figure 8 shows the top and bottom wall Nusselt numbers as functions of P_1, with P_2 as a parameter. For $P_2 = 0$ (vertical channel), the Nusselt number at both walls decreases gradually from the forced convection value of 8.235 as P_1 increases from zero. For nonzero P_2, the top wall Nusselt number at first decreases as P_1 increases, due to the flow deceleration at the top wall. Similarly, the bottom wall Nusselt number at first increases due to flow acceleration near the bottom. At $P_1 = 250$, both Nusselt numbers go to zero. They then increase as P_1 increases further, with the top wall Nusselt number now greater than the bottom wall Nusselt number, since flow reversal occurs at the bottom wall. The average Nusselt number (Fig. 9) behaves in a similar fashion, and approaches the vertical channel value as P_1 goes to infinity.

3.4 Dependence on Re, Gr, Pr and θ

By presenting the results as functions of the two parameters P_1 and P_2, some of the physical significance of the results is obscured. It is of interest to explore the effect of the more readily understandable parameters, *Re*, *Gr*, *Pr*, and θ. Figure 10 illustrates the routes through the P_1–P_2 plane which are followed if three of these parameters are held constant while the fourth is varied. If *Gr* is varied while the other parameters are held constant, a ray is followed out from

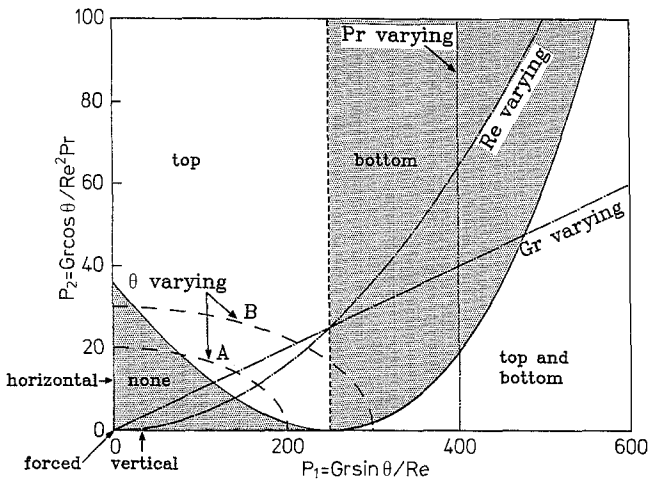

Fig. 10. Flow regimes: dependence on *Re*, *Gr*, *Pr*, θ

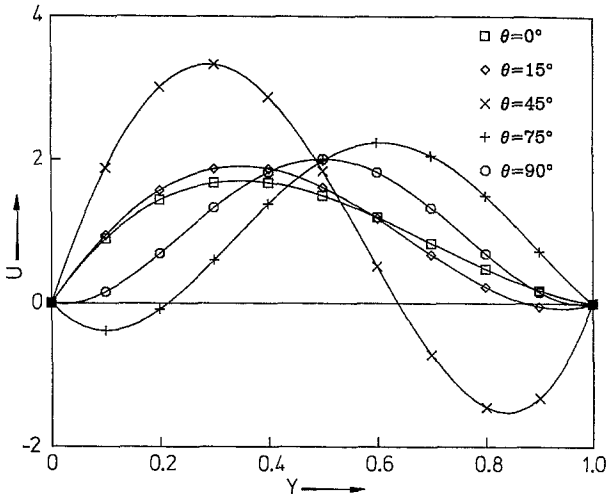

Fig. 12. Velocity profiles ($Re = 10$, $Gr = 3000$, $Pr = 1$)

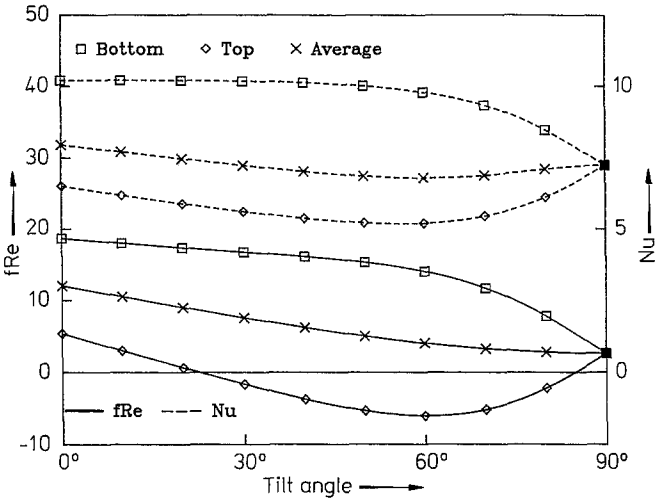

Fig. 11. fRe and Nu vs. tilt angle ($Re = 10$, $Gr = 2000$, $Pr = 1$)

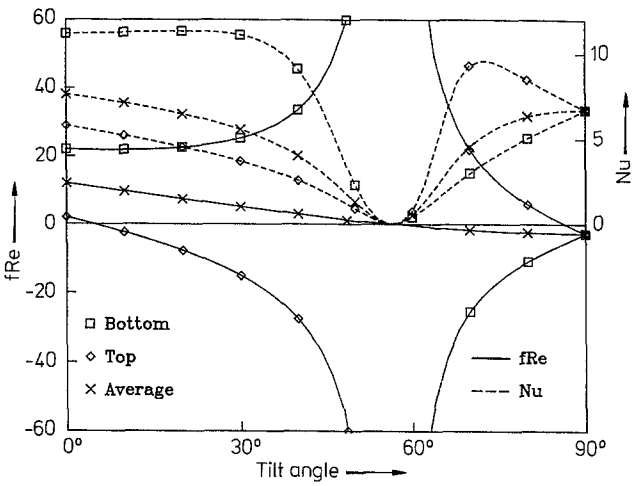

Fig. 13. fRe and Nu vs. tilt angle ($Re = 10$, $Gr = 3000$, $Pr = 1$)

the origin, that is $P_2 = C \cdot P_1$ where C is a constant which depends on the other parameters. In this case all four flow reversal regimes are traversed. If *Re* is varied while the other parameters are held constant, the curve $P_2 = D \cdot P_1^2$ is followed. As *Re* decreases from infinity ($P_1 = P_2 = 0$) at least three of the flow regimes are encountered, but whether or not the top and bottom flow reversal regime is entered depends on the values of the other parameters. If *Pr* is varied while the other parameters are held constant, then a line of constant P_1 is followed, so the sequence of flow reversal regimes depends on the value of P_1. If θ is varied while the other parameters are held constant, an ellipse $E \cdot P_1^2 + F \cdot P_2^2 = 1$ is followed. Two such curves are shown with dashed lines in Fig. 10. Clearly, it is possible to encounter various sequences of the flow reversal regimes, depending on the values of *Re*, *Gr*, and *Pr*.

These dashed curves, for varying θ, will now be investigated in more detail. The curve labelled *A* is for $Re = 10$, $Gr = 2000$, $Pr = 1$. As θ varies from 0 to 90 degrees (clockwise direction in Fig. 10), the flow regime changes from no reversal, to reversal at the top wall, back to no reversal. The wall friction and Nusselt numbers are illustrated in Fig. 11 as functions of tilt angle. The friction at the top wall becomes negative when flow reversal occurs, but the average wall friction remains positive. The shape of the Nusselt number curves is very similar to that of the wall friction. Note that the bottom wall friction and Nusselt number vary non-monotonically with θ, while the top wall and average value vary monotonically.

The dashed curve labelled *B* corresponds to $Re = 10$, $Gr = 3000$, $Pr = 1$. As θ varies from 0 to 90 degrees (clockwise direction), all four flow regimes are encountered. This is illustrated in Fig. 12, which shows the velocity profiles. For $\theta = 0$ degrees, there is no flow reversal. For $\theta = 15$ degrees there is a small reversal at the upper wall, and there is a larger reversal at the upper wall for $\theta = 45$ degrees. Flow

reversal occurs at the bottom wall for $\theta = 75$ degrees, and for $\theta = 90$ degrees there is flow reversal at both walls, although it is so small as to be invisible. Figure 13 shows the corresponding wall friction and Nusselt numbers as functions of tilt angle. The top and bottom wall frictions go to minus and plus infinity respectively, and then change sign and return from infinity when the transition from top to bottom flow reversal occurs (at $\theta = 56$ degrees). The average friction goes to zero at this point. The Nusselt numbers are seen to decrease to zero at the transition point and then increase again.

4 Concluding remarks

The exact solution has been derived for laminar opposing mixed convection between inclined parallel plates with a uniform wall heat flux boundary condition. The limiting cases of horizontal and vertical channels and forced convection can be recovered. The solution depends on the two parameters $P_1 = Gr \sin\theta / Re$ and $P_2 = Gr \cos\theta / Re^2 Pr$. Four different flow reversal regimes have been described and explored. They are 1) no reversal, 2) top reversal, 3) bottom reversal, and 4) top and bottom reversal. (More reversal regimes exist, but were not discussed because of their assumed instability). The dependence of the velocity and temperature profiles and the wall friction and heat transfer on the parameters P_1 and P_2 has been presented. The average wall friction was found to depend only on P_1. At $P_1 = 250$, the solution undergoes a discontinuous change between the top reversal and the bottom reversal regime. At this point, the top and bottom wall frictions go to plus or minus infinity, the average wall friction goes to zero, and the Nusselt numbers go to zero. The dependence on the four fundamental parameters *Re*, *Gr*, *Pr*, and θ has been briefly discussed. In particular, when θ is varied while holding the other three parameters constant, the sequence of flow regimes which is encountered depends on the values of *Re*, *Gr*, and *Pr*. The wall friction and Nusselt numbers may vary monotonically *or* nonmonotonically with tilt angle, again depending on the values of the other parameters, and on whether it is the top, bottom, or average value which is being considered.

The problem which has been solved is highly idealized: the predicted solution would probably be unstable for some ranges of the governing parameters. Furthermore, when flow reversal occurs, the fully developed condition can only exist very far from the inlet *and* the outlet, so that fully developed flow would not exist in many real systems. Despite the simplicity of the problem which has been analyzed, it does display some features which have been observed in real mixed convection flows, such as flow reversal and nonmonotonic dependence on tilt angle. The onset of the various flow reversal regimes in the present problem may indicate the presence of instability in a real system. As an example, consider Wirtz and McKinley's [4] experimental study of opposing mixed convection between vertical parallel plates. They reported that for $Re = 260$ and 560, the flow became unsteady at $Gr = 6.9 \times 10^4$ and 1.5×10^5, respectively. (These values have been converted to the definitions of *Re* and *Gr* used here.) These both correspond to $P_1 = 270$, which is quite close to the value of $P_1 = 250$ for which flow reversal is predicted to occur in a vertical channel. It should be noted that in Wirtz and McKinley's study, one plate was heated and the other was insulated. Due to radiation, there was some heat flux into the fluid at the insulated plate, and there was a decline in the heat flux near the end of the plates. Taking all of this into account does not change the conclusion that the experimental flow became unsteady at a value of P_1 very near the value at which flow reversal is predicted analytically.

The solution presented here may also prove useful as a guide for more complex numerical calculations. For instance, the existence of the discontinuous change (at $P_1 = 250$) in the solution presented here suggests a potential difficulty with the convergence of numerical calculations. If a similar discontinuous change occurs in a problem being studied numerically, then the numerical solution algorithm would probably not converge if it had to cross over this discontinuity. Therefore, care should be taken in choosing the initial flow field to be as close as possible to the final result.

It is hoped that the simple solution presented here will serve as a foundation for more complex and realistic studies of opposing mixed convection in inclined ducts or channels.

Acknowledgements

The author would like to acknowledge the helpful and illuminating discussions with Mr. Stanley Chen.

References

1. Gill, W. N.; Del Casal, E.: A theoretical investigation of natural convection effects in forced horizontal flows. AIChE J. 8 (1962) 513–518
2. Ostrach, S.: Combined natural- and forced-convection laminar flow and heat transfer of fluid with and without heat sources in channels with linearly varying wall temperatures. NACA TN 3141 (1954)
3. Cebeci, T.; Khattab, A. A.; LaMont, R.: Combined natural and forced convection in vertical ducts. Proc. 7th Int. Heat Transfer Conf. 3 (1982) 419–424
4. Wirtz, R. A.; McKinley, P.: Buoyancy effects on downwards laminar convection between parallel plates. Fundamentals of forced and mixed convection. ASME HTD 42 (1985) 105–112
5. Hallman, T. M.: Combined forced and free convection in a vertical tube. Ph.D. Thesis, Purdue Univ. 1958
6. Hanratty, T. J.; Rosen, E. M.; Kabel, R. L.: Effect of heat transfer on flow field at low Reynolds numbers in vertical tubes. Ind. Eng. Chem. 50 (1958) 815–820
7. Morton, B. R.: Laminar convection in uniformly heated pipes. J. Fluid Mech. 8 (1960) 227–240
8. Scheele, G. F.; Hanratty, T. J.: Effect of natural convection on stability of flow in a vertical pipe. J. Fluid Mech. 14 (1962) 244–256

9. Collins, M. W.: Heat transfer by laminar combined convection in a vertical tube. – Predictions for water. Proc. 6th Int. Heat Transfer Conf. 1 (1978) 25–30
10. Bohne, D.; Obermeier, E.: Combined free and forced convection in a vertical and inclined cylindrical annulus. Proc. 8th Int. Heat Transfer Conf. 3 (1986) 1401–1406
11. Lavine, A. S.; Shores, C. N.; Kim, M. Y.: Flow reversal in mixed convection flow in inclined pipes. ASME Paper no. 86-WA/HT-79 (1986)
12. Lavine, A. S.; Kim, M. Y.; Shores, C. N.: Reversal in mixed convection in inclined pipes. – Stability characteristics. Proc., 1987 ASME/JSME Thermal Eng. Conf. 3 (1987) 645–652
13. Choudhury, D.; Patankar, S. V.: Developing laminar flow and heat transfer in the entrance region of an inclined isothermal tube. ASME Paper no. 86-WA/HT-87 (1986)

Adrienne S. Lavine, Assistant Professor
Mechanical, Aerospace and Nuclear Engineering Department
University of California, Los Angeles
Los Angeles, CA 90024, USA

Received December 23, 1987